Journal of Power Sources 273 (2015) 544–553

Contents lists available at ScienceDirect

Journal of Power Sources

journal homepage: www.elsevier.com/locate/jpowsour

Novel sulfonated poly (ether ether ketone)/phosphonic acid-functionalized titania nanohybrid membrane by an *in situ* method for direct methanol fuel cells

Hong Wu [a, b, c], Ying Cao [a, b], Zhen Li [a, b], Guangwei He [a, b], Zhongyi Jiang [a, b, *]

[a] Collaborative Innovation Center of Chemical Science and Engineering (Tianjin), Tianjin 300072, China
[b] Key Laboratory for Green Chemical Technology, School of Chemical Engineering and Technology, Tianjin University, Tianjin 300072, China
[c] Tianjin Key Laboratory of Membrane Science and Desalination Technology, Tianjin University, Tianjin 300072, China

HIGHLIGHTS

- Phosphonic acid-modified titania nanoparticles were *in situ* synthesized in SPEEK.
- The hybrid membranes had good nanoparticle dispersion and interfacial morphology.
- Extra proton conduction sites and well-connected channels were introduced in SPEEK.
- The hybrid membrane showed enhanced proton conductivity up to 0.334 S cm^{-1}.

ARTICLE INFO

Article history:
Received 21 June 2014
Received in revised form
14 September 2014
Accepted 21 September 2014
Available online 30 September 2014

Keywords:
Phosphonic acid
In situ sol–gel process
Titania
Sulfonated poly (ether ether ketone)
Nanohybrid membranes
Proton conductivity

ABSTRACT

Sulfonated poly (ether ether ketone)/phosphonic acid-functionalized titania nanohybrid membranes are prepared by an *in situ* method using titanium tetrachloride ($TiCl_4$) as inorganic precursor and amino trimethylene phosphonic acid (ATMP) as modifier. Phosphonic acid-functionalized titania nanoparticles with a uniform particle size of ~50 nm are formed and dispersed homogeneously in the SPEEK matrix with good interfacial compatibility. Accordingly, the nanohybrid membranes display remarkably enhanced proton conduction property due to the incorporation of additional sites for proton transport and the formation of well-connected channels by bridging the hydrophilic domains in SPEEK matrix. The nanohybrid membrane with 6 wt. % of phosphonic acid-functionalized titania nanoparticles exhibits the highest proton conductivity of 0.334 S cm^{-1} at 65 °C and 100% RH, which is 63.7% higher than that of pristine SPEEK membrane. Furthermore, the as-prepared nanohybrid membranes also show elevated thermal and mechanical stabilities as well as decreased methanol permeability.

1. Introduction

Direct methanol fuel cells (DMFCs) have attracted extensive attention as promising clean power sources for decades [1–4]. Proton exchange membranes (PEMs) are one of the core components of DMFCs [5–7]. In recent years, enormous efforts have been dedicated to developing PEMs based on phosphonic acid groups as alternative proton conductors for DMFCs applications [8–10]. The amphoteric phosphonic acid groups can facilitate proton conduction by forming dynamical hydrogen bond networks [11,12]. Compared with sulfonic acid groups, phosphonic acid groups show lower energy penalty in transferring protons (37.2 kJ mol^{-1} and 69.9 kJ mol^{-1} for phosphonic acid and sulfonic acid groups, respectively) and higher water bonding energy (47.3 kJ mol^{-1} and 44.4 kJ mol^{-1} for phosphonic acid and sulfonic acid groups, respectively), where the former promotes proton transport and the latter renders enhanced water retention property [13–15]. To develop phosphonic acid-based membranes, phosphonic acid groups are either anchored on the polymer chains or directly doped into polymer matrix [9,10]. However, these types of membranes suffer from either the complicated synthesis procedure or the severe leakage of phosphonic acids in hydrated state [16]. It is believed that incorporating inorganic particles with covalently bonded phosphonic acid groups into polymer matrix can effectively suppress the undesirable leaching, meanwhile retain the advantages of the low methanol permeability and high mechanical stability from inorganic materials [17].

* Corresponding author. School of Chemical Engineering and Technology, Tianjin University, Tianjin 300072, China. Tel./fax: +86 022 23500086.
E-mail address: zhyjiang@tju.edu.cn (Z. Jiang).

http://dx.doi.org/10.1016/j.jpowsour.2014.09.134
0378-7753/

For the preparation of organic-inorganic hybrid membranes, the size of inorganic particles usually has crucial influence on membrane properties [18–21]. Micron-sized inorganic particles might cause some non-ideal effects at the organic–inorganic interface in hybrid membrane, whereas nano-sized inorganic particles with higher surface area could enhance the polymer-filler compatibility and provide more reaction sites for further functionalization. Inorganic particles smaller than 100 nm in diameter are more preferred as fillers to improve membrane performance [20,22]. Nevertheless, inorganic fillers with large particle sizes are often utilized in the preparation of hybrid membranes through physical blending method, because nanoparticles smaller than 100 nm in diameters are difficult to prepare and they often tend to aggregate in membranes [23]. Alternatively, preparing the hybrid membranes by *in situ* method, through which inorganic nanoparticles are formed within polymer matrix during the membrane casting process, can overcome afore mentioned problems [24,25]. In this method, the hydrolysis and condensation reactions of inorganic precursors take place in polymer matrix, thus the formation of inorganic nanoparticles is confined in polymeric network, resulting in homogeneous particle distribution without aggregation [26,27]. Moreover, the size and the amount of inorganic nanoparticles can be controlled by adjusting the preparation conditions (the concentration of inorganic precursor, the reaction temperature, *etc.*) in *in situ* method [25]. Inorganic nanoparticles such as titania [28], silica [29,30] and zeolite [31] have been *in situ* incorporated into Nafion and other polymers with microphase separation behavior to fabricate hybrid membranes [32]. Such prepared membranes exhibit good interfacial compatibility as well as enhanced water retention property and mechanical stability [29,30]. As we know, acid-functionalized nanoparticles are favorable to increase proton conductivity due to their ability to bridge the hydrophilic domains of polymers [20], and their high surface area enables high loading of acid groups [33]. However, since too fast a rate of sol–gel reaction will cause heterogeneity in hybrid membranes, more controllable methods remain to be explored [34]. Hybrid membranes embedded with *in situ* formed sulfonic acid-functionalized nanoparticles are intensively studied [29,30], whereas few efforts have been dedicated to those embedded with *in situ* formed phosphonic acid-functionalized nanoparticles [18,35]. Theoretically, *in situ* method is an effective approach to introduce phosphonic acid-functionalized nanoparticles into polymer matrix for improving the performance of PEMs.

In this study, a novel hybrid membrane is developed with sulfonated poly (ether ether ketone) (SPEEK) as polymer matrix and nano-sized phosphonic acid-functionalized titania as fillers. The prepared hybrid membranes are expected to have enhanced proton conductivity along with reduced methanol permeability. Herein, the titania nanoparticles are prepared from titanium tetrachloride ($TiCl_4$) by *in situ* sol–gel method and functionalized with amino trimethylene phosphonic acid (ATMP) by covalent bonds. The formation of titania nanoparticles and the graft of phosphonic acid occur simultaneously during membrane fabrication. The as-prepared hybrid membranes are characterized by FTIR, XPS, SEM, XRD and TGA, while the membranes performance are extensively evaluated in terms of mechanical stability, water uptake, swelling degree, methanol permeability and proton conductivity.

2. Experimental

2.1. Materials and chemicals

Poly (ether ether ketone) (PEEK) was supplied by Victrex High-performance Materials Co., Ltd. (Shanghai, China). Titanium tetrachloride ($TiCl_4$, ≥99 wt. %) was purchased from Tianjin Suzhuang Chemical Reagent Factory (Tianjin, China). Amino trimethylene phosphonic acid (ATMP) was purchased from Shandong Taihe Water Treatment Co., Ltd. *N*,*N*-Dimethylformamide (DMF, >99.5%), hydrochloric acid (HCl, 36–38%) and sulfuric acid (H_2SO_4, 95–98%) purchased from Tianjin Guangfu Fine Chemical Research Institute (Tianjin, China) were of chemical reagent grade and were used as received.

2.2. Sulfonation of PEEK

Sulfonated poly (ether ether ketone) (SPEEK) was synthesized by direct sulfonation of PEEK [36]. PEEK was dried overnight at 80 °C before sulfonation. 28 g of dried PEEK was dissolved in 200 mL of concentrated sulfuric acid (H_2SO_4, 95–98%) under continuous stirring. The sulfonation reaction was performed at room temperature for 3 h and then at 45 °C for 8 h. After cooling to room temperature, the resultant mixture was poured out slowly into ice water to get precipitation, which was then washed with deionized water until neutral pH. The obtained SPEEK was dried under room temperature for 24 h and then at 60 °C under vacuum until constant weight was achieved. The sulfonation degree (DS) of SPEEK was measured to be 68% by acid-base titration.

2.3. Membrane preparation

Firstly, 0.65 g SPEEK was dissolved in 6 mL DMF at room temperature and stirred for 24 h. Simultaneously, a certain amount of $TiCl_4$ was added into a 2:1 (v:v) water-ethanol mixture dropwise and stirred continuously for 2 h, then the resultant homogenous sol was added into SPEEK–DMF solution drop by drop and stirred for another 2 h. Subsequently, a measured amount of ATMP was dissolved in 2 mL DMF, and added into above mixture (the molar ratio of $TiCl_4$ to ATMP was 4:1). After stirred for 1 h, the obtained casting solution was poured onto a clean glass plate and heated in oven at 60 °C for 12 h, and then heated at 80 °C for another 12 h to remove the solvent completely. The membranes were peeled off and immersed in 2 M HCl solution to convert the membranes into required acid form. Finally, the membranes were washed with deionized water until neutral pH was obtained to remove residual acid and possible impurities. The resultant hybrid membranes were designated as SPEEK/TOLP-*X*. The preparation procedure is shown in Scheme 1. Hybrid membranes without ATMP were also prepared using similar procedure without the addition of ATMP–DMF solution, and denoted as SPEEK/TOL-*X*. The TiO_2 weight proportions *X* were given assuming total conversion of $TiCl_4$ to titania.

2.4. Characterization

Fourier transform infrared spectra (FTIR, 4000–400 cm^{-1}) were carried out on a Nicolet MAGNA-IR 560 instrument to determine the chemical composition of $TiCl_4$ sol. X-ray photoelectron spectroscopy (XPS) was employed to examine the chemical composition of membranes using a PHI-1600 spectrometer with Al Kα radiation for excitation.

The microstructure of cross-sectional morphology of the as-prepared membranes was examined by field emission scanning electron microscopy (FESEM, Nanosem 430) operated at 20 kV. The samples were prepared by freeze-fracturing in liquid nitrogen, and subsequently coated with a thin layer of sputtered gold. The distribution of titanium and phosphorus in membranes was observed by energy dispersive spectrometer (EDS).

The nanostructure of pristine SPEEK and hybrid membranes was investigated by X-ray diffraction scattering (XRD) operated on a Rigaku D/max 2500 V/PC instrument in an angular range of 5–80° with a scan rate of 5° min^{-1}.

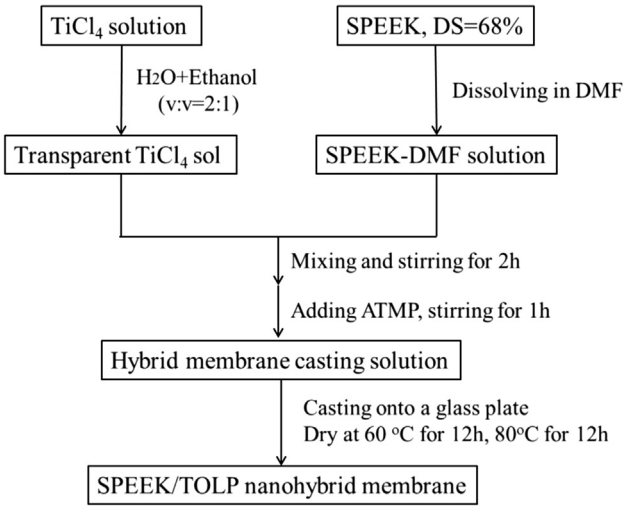

Scheme 1. Preparation procedure of SPEEK/TOLP hybrid membranes.

Thermogravimetric analysis (TGA, Perkin–Elmer Pyris) of membranes was recorded in the temperature range of 30–800 °C with a heating rate of 10 °C min^{-1} under N_2 atmosphere, and all the membranes were dried overnight under vacuum before test.

The mechanical properties of the as-prepared membranes were investigated using a WDW-02 test machine with an elongation rate of 10 mm min^{-1} at room temperature. The samples were prepared by cutting membranes into 1.0 × 4.0 cm strips.

2.5. Water uptake and swelling degree

Pieces of rectangular-shaped membrane samples were dried at 80 °C in an oven for 24 h, then their weights (W_d, g) and areas (A_d, cm^2) were measured. Afterward, the membrane samples were immersed in 25 °C water for 24 h, and the weights (W_w) and areas (A_w) of wet membranes were measured again. The water uptake and swelling degree were calculated by the following equations:

$$\text{water uptake}\ (\%) = \frac{W_w - W_d}{W_d} \times 100\% \quad (1)$$

$$\text{swelling degree}\ (\%) = \frac{A_w - A_d}{A_d} \times 100\% \quad (2)$$

The swelling degree of membranes was measured in both in-plane direction and through-plane direction. The areas in Equation (2) were obtained by multiplying the length by the width of membrane for in-plane swelling, and multiplying the width by the thickness of membrane for through-plane swelling.

2.6. Methanol permeability

In methanol permeability measurement, a glass diffusion cell composed of two compartments with an identical volume of 30 mL was used. Before test, membrane samples were soaked in water for 24 h to be fully hydrated. Membrane samples were placed vertically between the two compartments, which were subsequently filled with water (compartment A) and 2 M methanol solution (compartment B). The amount of methanol diffused from compartment B to compartment A across the membrane over time was measured by a gas chromatography (Agilent 7820) equipped with a thermal conductivity detector (TCD) and a DB-624 column. During the test, both compartments were stirred continuously. The methanol permeability was calculated using the following equation.

$$P\left(\text{cm}^2\ \text{s}^{-1}\right) = S\frac{V_A L}{AC_{B0}} \quad (3)$$

where S is the slope of the straight line of methanol concentration versus time in compartment A, and V_A (mL) is the volume of the receipt compartment. L (cm) and A (cm^2) are the thickness and diffusion area of membranes respectively. C_{B0} (mol mL^{-1}) is the initial concentration of methanol in compartment B.

2.7. Proton conductivity

Proton conductivity of the as-prepared membranes in horizontal direction was measured using the AC impedance spectroscopy analyzer with an electrochemical workstation (Princeton Parstat 2273 Electrochemical System) over a frequency range of 1–10^6 Hz at voltage amplitude of 20 mV. Membrane samples were soaked in 25 °C deionized water for at least 48 h to be fully hydrated before measurement. Membrane samples were sandwiched in the two-point-probe cell and heated with water vapor. The measurement was performed at the temperature range of 20–65 °C and 100% relative humidity. Each membrane was measured for three times. The proton conductivity was calculated as follow.

$$\sigma\left(\text{S cm}^{-1}\right) = \frac{l}{AR} \quad (4)$$

where l (cm) is the distance between the two electrodes, A (cm^2) is the cross-sectional area of the membrane, and R (Ω) is the resistance derived from the low intersection of the high frequency semicircle on a complex impedance plane with Re (z) axis.

3. Results and discussion

3.1. Characterization of $TiCl_4$ sol

During the membrane preparation process, $TiCl_4$ was added into ethanol–water solution dropwise at room temperature. After stirred for 2 h, a light yellow solution was obtained. When ATMP was added directly into such a solution, white precipitate generated rapidly. The FTIR spectra of both $TiCl_4$ sol and the white precipitate are shown in Fig. 1. In the presence of ATMP, a weak peak appears at 576 cm^{-1} is attributed to the Ti–O–Ti stretching vibration,

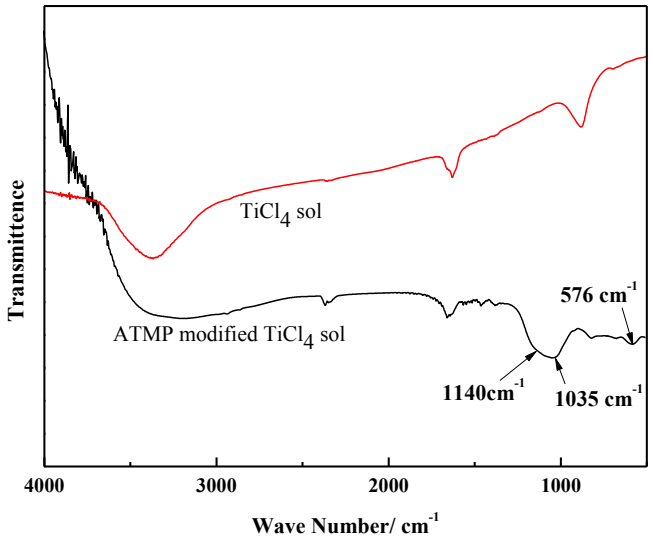

Fig. 1. FTIR spectra of $TiCl_4$ sol and ATMP modified $TiCl_4$ sol.

confirming the formation of titania. The strong peaks at 1035 cm^{-1} and 1140 cm^{-1} are assigned respectively to the stretching vibration of P–O–Ti and P═O, indicating that covalent bonds are formed between titanium atoms and phosphate groups through chemical adsorption [17]. Thus it is reasonable to deduce that ATMP can facilitate the hydrolysis of $TiCl_4$. In this regard, ATMP was added after the mixing process of $TiCl_4$ sol and SPEEK solution in order to obtain nanohybrid membranes with uniformly dispersed inorganic fillers.

3.2. Characterization of membranes

In order to confirm the chemical status of Ti and P in membranes, XPS analysis was conducted on both SPEEK/TOL and SPEEK/TOLP hybrid membranes. Fig. 2(a) shows the overall XPS spectra of these two kinds of hybrid membranes. The O 1s, Ti 2p and C 1s peaks are observed in the spectrum of SPEEK/TOL hybrid membrane, while an additional peak assigned to P 2p appears in the spectrum of SPEEK/TOLP hybrid membrane. To further confirm the

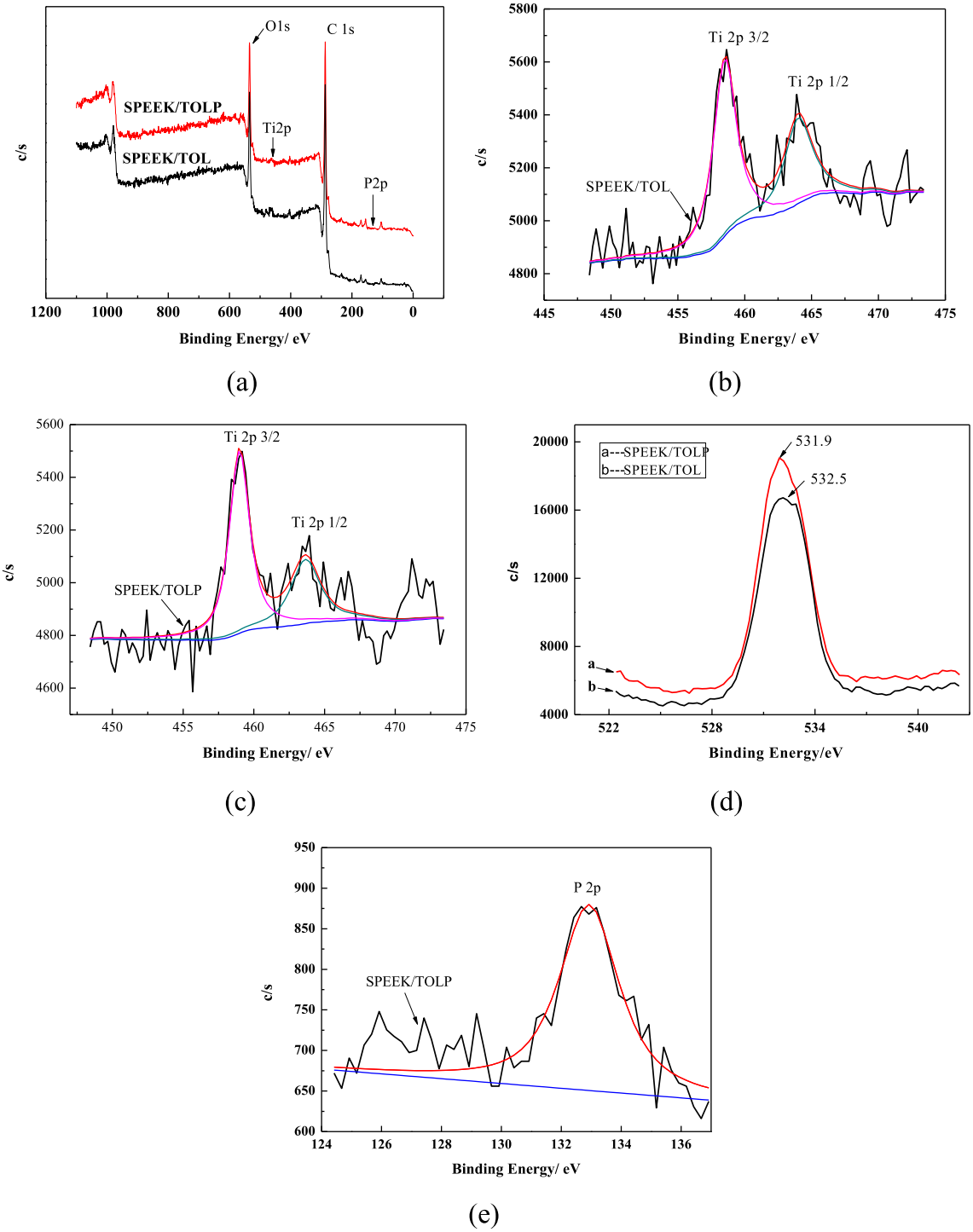

Fig. 2. Overall XPS spectra of SPEEK/TOL and SPEEK/TOLP (a), XPS spectra of Ti 2p of SPEEK/TOL (b) and SPEEK/TOLP (c), O 1s of SPEEK/TOL and SPEEK/TOLP (d), P 2p of SPEEK/TOLP (e).

chemical composition of these hybrid membranes, peak-differentiating-imitating analysis was conducted for each element and the resultant spectra are shown in Fig. 2(b)–(e). For both kinds of the as-prepared hybrid membranes, the main Ti $2p_{3/2}$ components of the Ti 2p doublets exhibit a peak at 458.9 eV, representing the O–Ti–O type chemical environment (see Fig. 2(b) and (c)). This result is consistent with the XPS spectra of TiO_2 particles prepared *via* sol–gel method [37], confirming the successful formation of titania within membranes. The O 1s spectrum at 532.5 eV for the SPEEK/TOL hybrid membrane corresponds to the C–O–Ti state (Fig. 2(d)). For the SPEEK/TOLP hybrid membrane, the binding energy of O 1s is 531.9 eV, which is consistent with that of oxygen in the Ti–O–P and P=O environment. Besides, as shown in Fig. 2(e), the P 2p peak at 132.8 eV for phosphonic acid-doped membrane confirms the presence of P–O bond [38]. The above results confirm the successful phosphorylation of titania with ATMP.

SEM images of the cross-section of the pristine SPEEK and hybrid membranes are presented in Fig. 3. For all the hybrid membranes, titania particles with a uniform particle size of about 50 nm are generated and dispersed homogeneously within the

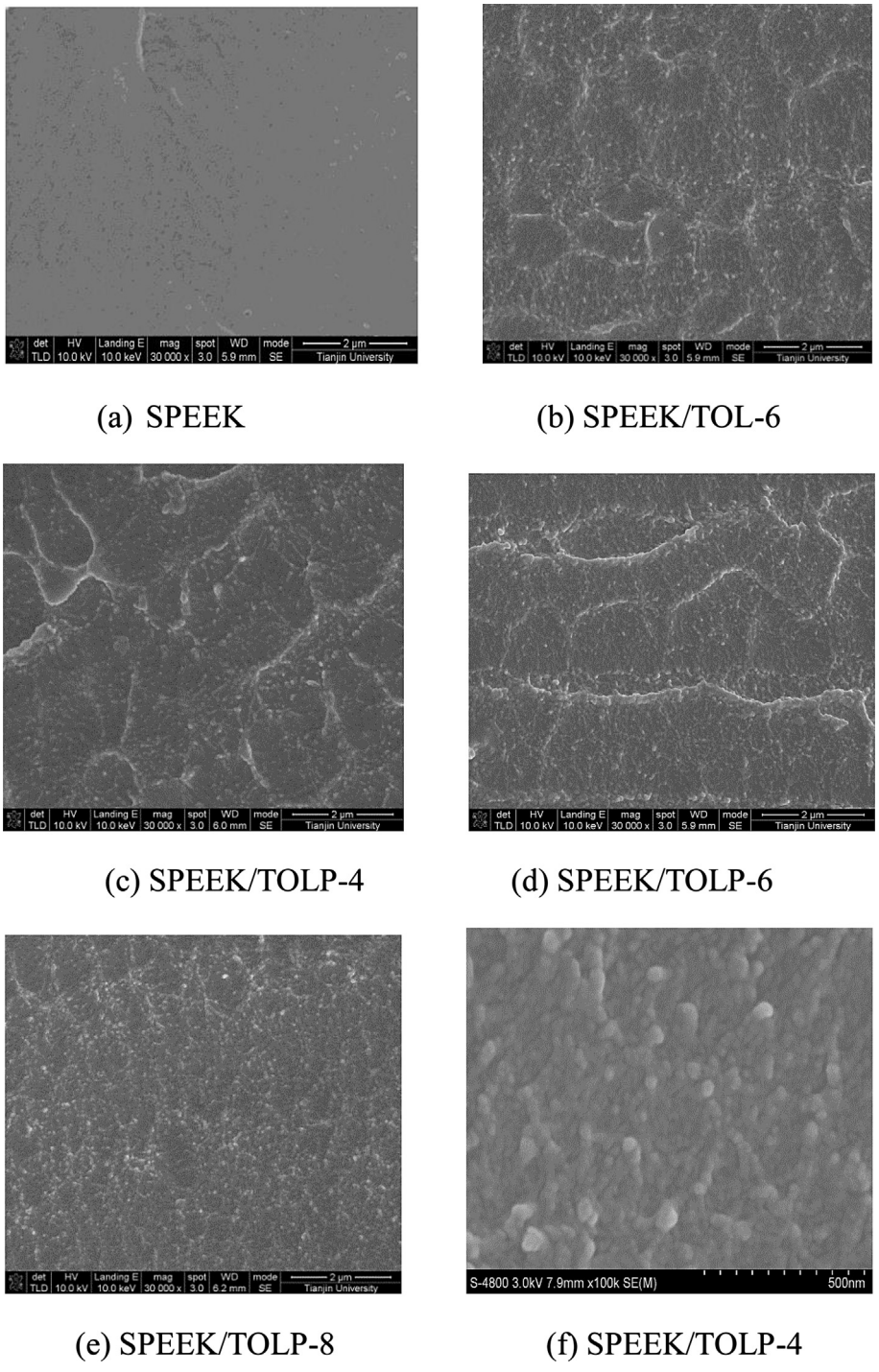

Fig. 3. SEM images of the cross-section of pristine SPEEK and hybrid membranes.

SPEEK matrix. The hydrolysis and condensation reactions of $TiCl_4$ are restricted by the polymeric network during membrane formation. With the increase of the $TiCl_4$ concentration, more titania nanoparticles are generated in polymer matrix. The incorporation of ATMP in the mixture of $TiCl_4$ sol and SPEEK solution do not cause non-uniform morphology of SPEEK/TOLP hybrid membranes. For all the as-prepared membranes, no obvious structural defects are observed, hinting that no phase separation occurs during the preparation process. This result reveals that the interaction between SPEEK and titania nanoparticles/organics grafted on titania nanoparticles has improved the interfacial compatibility between the polymer matrix and the inorganic fillers.

Fig. 4(a) is the backscatter electron image of SPEEK/TOLP-6 membrane and Fig. 4(b) is the corresponding EDS spectrum, which shows clear peaks of P and Ti. The distribution of titanium and phosphorus elements is confirmed by EDS-mapping. As shown in Fig. 4(c) and (d), both titanium and phosphorus distribute homogeneously within the membrane, and the distribution of phosphorus is in good agreement with that of titanium, indicating that phosphonic acid groups are attached on titania and the nanoparticles are well introduced into SPEEK.

The XRD patterns of the pristine SPEEK and hybrid membranes are presented in Fig. 5. PEEK is reported to be a semicrystalline polymer with sharp crystalline peaks in the 2θ range of 20–30° [39], and its crystallinity will be strongly decreased after sulfonation [40]. From the XRD profile, it can be seen that there is a broad crystalline peak overlays on the 2θ range of 20–25° for the pristine SPEEK membrane, indicating that SPEEK is a polymer with low crystallinity. Both SPEEK/TOL and SPEEK/TOLP hybrid membranes show broad peaks at the same location just as the pristine SPEEK membrane, whereas the peak intensity is slightly lower. The reduction in intensity reveals that the *in situ* formed titania nanoparticles induce disorder of SPEEK structure and result in decreased crystallinity of hybrid membranes. As the concentration of $TiCl_4$ is increased, more titania nanoparticles are generated in SPEEK matrix, leading to further decreased crystallinity.

3.3. Thermal stability of membranes

The effect of *in situ* formed titania nanoparticles on thermal stability of hybrid membranes was investigated by thermogravimetric analysis (TGA). The TGA curves of pristine SPEEK and hybrid membranes are shown in Fig. 6. For all membranes, the TGA curves exhibit three main degradation stages. The first weight loss in the temperature range of 30–150 °C is attributed to the evaporation of absorbed water in the membranes. The second weight loss between 300 and 400 °C is assigned to the decomposition of sulfonic acid groups of SPEEK and organic functional groups introduced to titania nanoparticles. The last weight loss start from 450 °C is ascribed to the degradation of SPEEK main chains [41]. For hybrid membranes, the degradation temperatures in the second and third stages are slightly increased, and tend to be higher with the increase of filler content. One possible explanation is that the microstructure of hybrid membranes is affected by the interaction

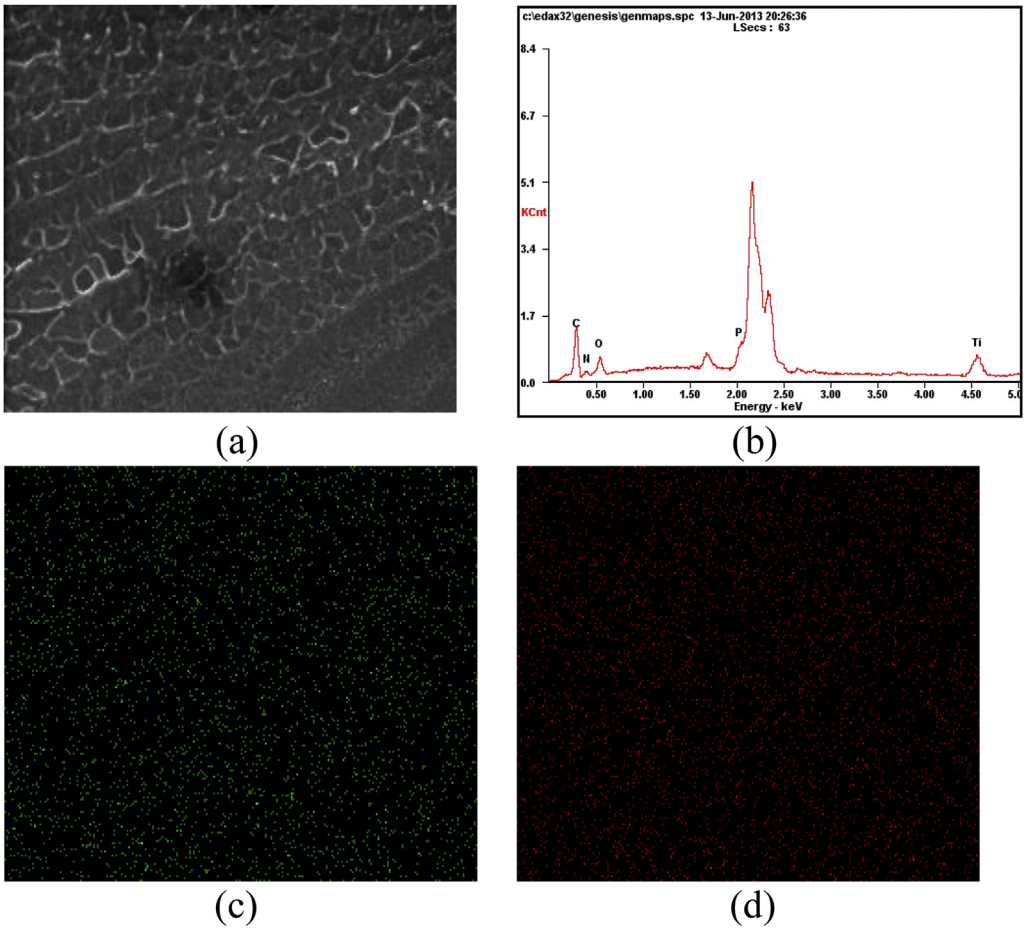

Fig. 4. Backscattered electron image of SEM (a) and corresponding EDX spectrum (b) of the SPEEK/TOLP-6 hybrid membrane, EDS-mapping of Ti (c), and P (d) of SPEEK/TOLP-6 hybrid membrane.

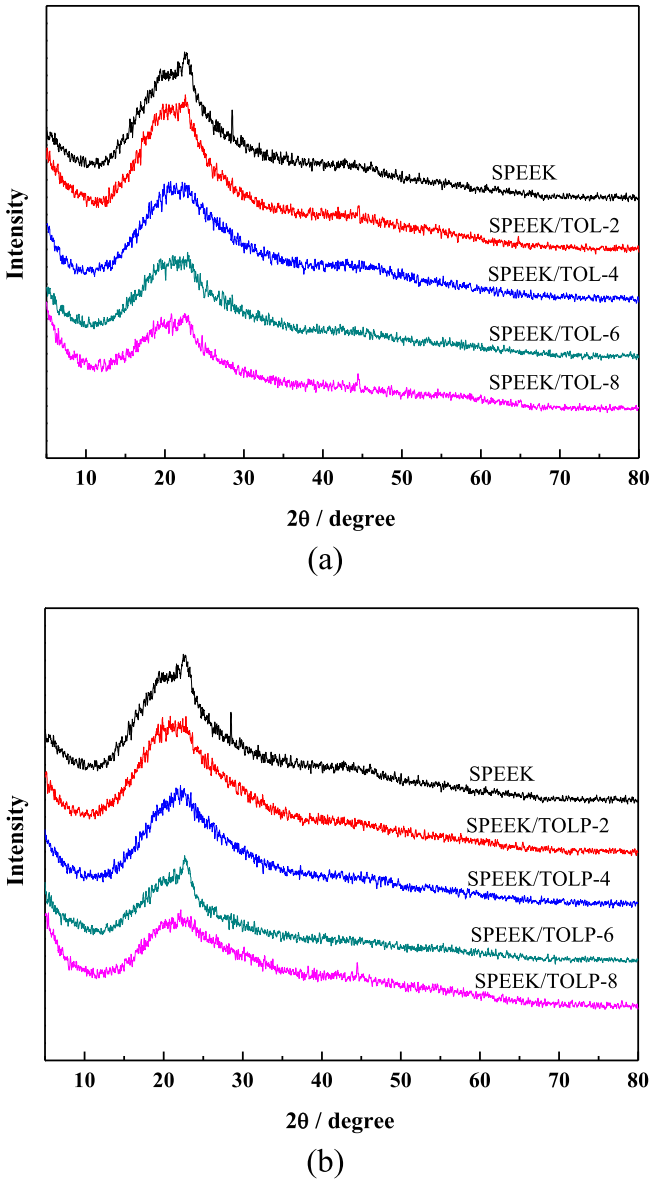

Fig. 5. XRD spectra of the pristine SPEEK membrane and SPEEK/TOL (a), SPEEK/TOLP hybrid membranes (b).

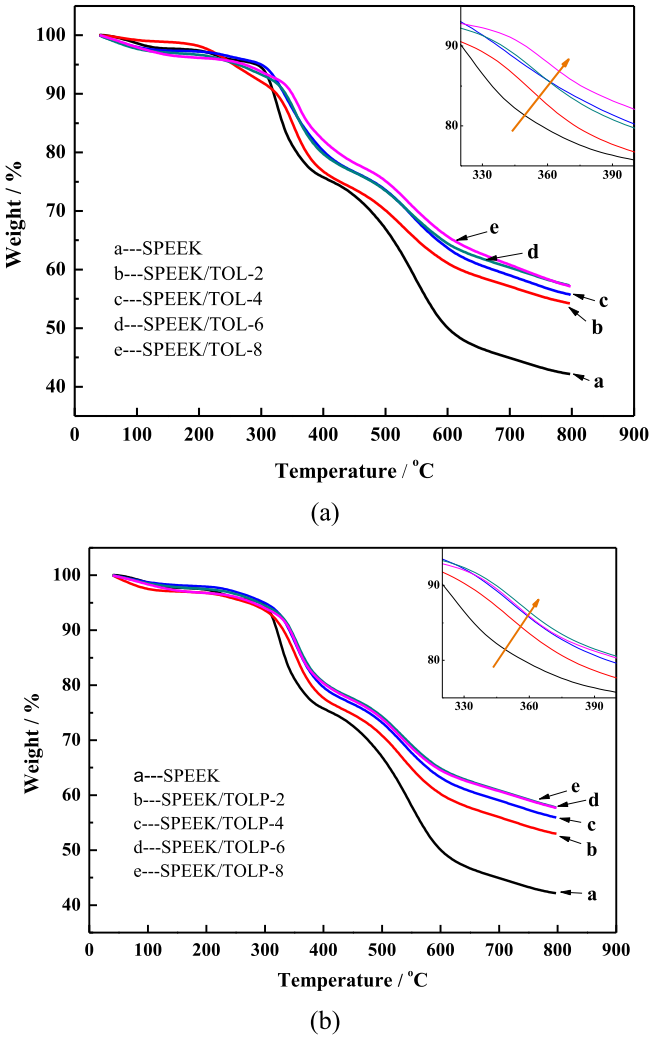

Fig. 6. TGA curves of the pristine SPEEK membrane and SPEEK/TOL (a), SPEEK/TOLP hybrid membranes (b).

between titania nanoparticles and SPEEK matrix, resulting in enhanced thermal stability. In the temperature range of 300–400 °C, the degradation temperature of SPEEK/TOLP hybrid membrane is slightly higher than that of SPEEK/TOL hybrid membrane. This result suggests that the incorporation of ATMP further increases the interaction between organic phase and inorganic phase, thus endowing SPEEK/TOLP hybrid membrane with better thermal stability than SPEEK/TOL hybrid membrane. Besides, all the hybrid membranes present good thermal stability below 250 °C, meeting the requirement of practical application in DMFCs.

3.4. Mechanical stability of membranes

The mechanical properties of the as-prepared membranes were evaluated in terms of tensile test, and the obtained stress–strain curves are presented in Fig. 7. The tensile strength is the stress taken at the maximum of the stress–strain curve while the ductility is expressed as the percentage of elongation at fracture. The tensile

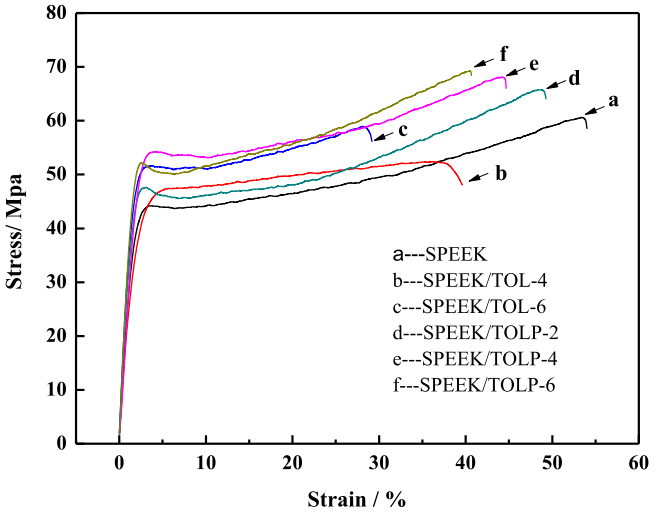

Fig. 7. The stress–strain curves of pristine SPEEK membrane, SPEEK/TOL and SPEEK/TOLP hybrid membranes.

strength and elongation at fracture of pristine SPEEK membrane are measured to be 61 Mpa and 54% respectively, which are consistent with those reported in literature [42]. After the incorporation of unmodified titania nanoparticles, the tensile strength of hybrid membranes is decreased due to the perturbed balance of weak and strong regions of SPEEK caused by structural inhomogeneity [42]. On the contrary, the SPEEK/TOLP hybrid membranes show increased tensile strength compared with pristine SPEEK membrane, resulting from the enhanced intermolecular forces (electrostatic force and hydrogen bonds between phosphonic acid groups on titania and sulfonic acid groups on SPEEK) between polymer chains. The elongations of both SPEEK/TOL and SPEEK/TOLP hybrid membranes are lower than that of pristine SPEEK membrane and decrease with the increase of filler content. The reduced ductility of these hybrid membranes can be due to the incorporation of rigid inorganic fillers blocks the movement of polymer chains [43]. Nevertheless, the elongations of SPEEK/TOLP hybrid membranes with filler contents lower than 6 wt. % are still higher than 40%, flexible enough to be used as PEMs in DMFCs.

3.5. Water uptake and swelling degree

The water uptake and swelling degree of the pristine SPEEK and hybrid membranes are shown in Fig. 8. For the pristine SPEEK membrane, the water uptake is measured to be 49 wt. % (Fig. 8(a)), and the swelling degree in in-plane direction and through-plane direction are 33.7% and 26.4%, respectively (Fig. 8(b)). For SPEEK/TOL and SPEEK/TOLP hybrid membranes, the water uptake and swelling degree (in both in-plane and through-plane direction) are lower than those of pristine SPEEK membrane and decrease with the increase of filler content. The decreased water uptake of hybrid membranes is related to the less hydrophilic character of the *in situ* formed titania nanoparticles compared with SPEEK and the reduced molecular empty space in polymer matrix available for water molecules entrance, which are also responsible for the decreased swelling degree. Another reason for the decrease of swelling degree may be the incorporation of titania nanoparticles which can restrict the movement of polymer chains. Both the water uptake and swelling degree of SPEEK/TOLP hybrid membranes are higher than those of SPEEK/TOL hybrid membranes since the phosphonic acid groups on titania nanoparticles endow the former kind of hybrid membranes with enhanced hydrophilic property. In addition, for SPEEK/TOLP hybrid membrane with 6 wt. % filler content, the in-plane swelling is reduced by 17% and the through-plane swelling is reduced by 25% compared with those of pristine SPEEK membrane. The larger change of swelling in through-plane direction than that of in-plane direction indicates that the incorporation of *in situ* formed titania nanoparticles is more effective in restricting membrane swelling in proton transport direction.

3.6. Methanol permeability

Methanol permeability is one of the most important parameters to determine the comprehensive performance of membranes for DMFCs. The methanol permeability measurement of the as-prepared membranes was carried out in a 2 mol L^{-1} methanol solution at room temperature and the results are presented in Fig. 9. The measured methanol permeability of pristine SPEEK membrane is 7.25×10^{-7} cm^2 s^{-1}. After the incorporation of *in situ* formed titania, the methanol permeability of both SPEEK/TOL and SPEEK/TOLP hybrid membranes is reduced and decreased with the increase of filler content. As the content of titania nanoparticles increases from 2 wt. % to 8 wt. %, the methanol permeability decreases from 6.44×10^{-7} cm^2 s^{-1} to 4.98×10^{-7} cm^2 s^{-1} for SPEEK/TOL hybrid membranes and from 6.52×10^{-7} cm^2 s^{-1} to 5.30×10^{-7} cm^2 s^{-1} for SPEEK/TOLP hybrid membranes. The presence of titania nanoparticles provides tortuous pathways for methanol transport, and the lower water uptake of hybrid membranes allows less methanol to pass through along with water, thereby restricting the methanol crossover. At the same filler content, the membranes incorporated with phosphonic acid-functionalized titania nanoparticles exhibit slightly higher methanol permeability as compared with those incorporated with pristine titania nanoparticles.

3.7. Proton conductivity

Proton conductivity is the fundamental and key index to evaluate PEMs for potential use in DMFCs. The proton transport mechanism can be described either by “vehicular mechanism” or by “Grotthus mechanism” [44]. In the former mechanism, protons are attached to water to form hydronium ions (e.g. H_3O^+ and $H_5O_2^+$), which can diffuse as a whole through membranes. For the later mechanism, protons are transferred by means of hopping from one

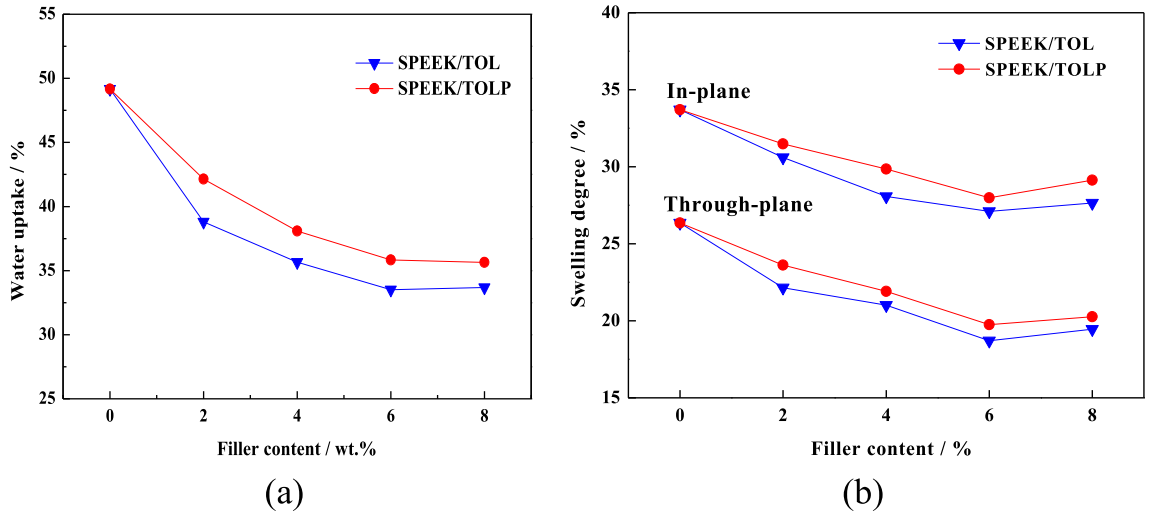

Fig. 8. The water uptake (a), and swelling degree in in-plane and through-plane direction (b) of pristine SPEEK, SPEEK/TOL and SPEEK/TOLP hybrid membranes at room temperature.

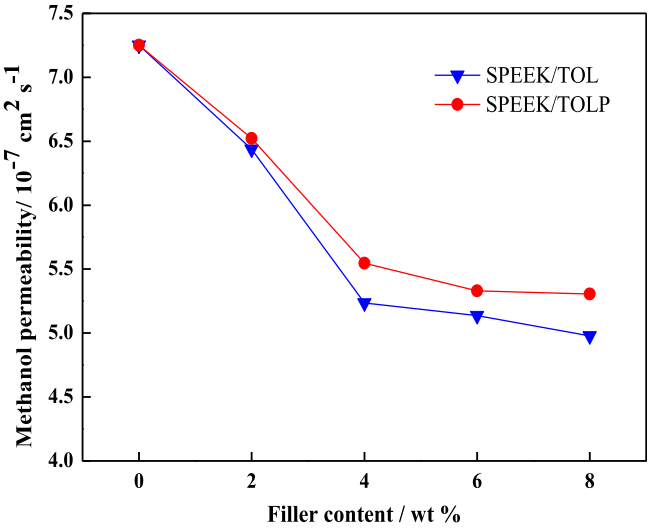

Fig. 9. The methanol permeability of pristine SPEEK, SPEEK/TOL and SPEEK/TOLP hybrid membranes at room temperature.

proton-conducting site to another with continuous forming and breaking of hydrogen bonds. The proton conductivity of the pristine SPEEK and hybrid membranes as a function of temperature at 100% RH was tested and the result is shown in Fig. 10. The proton conductivity of pristine SPEEK membrane increases from 0.079 S cm^{-1} to 0.210 S cm^{-1} as the temperature is increased from 20 °C to 60 °C, and afterward decreases at higher temperatures. In comparison, the proton conductivity of all the hybrid membranes increases monotonously with temperature in the experimental range of 20–65 °C, suggesting that the proton conduction is a thermally activated process in the hybrid membranes. For the SPEEK/TOL hybrid membranes, the proton conductivity is lower than that of pristine SPEEK membrane at the same temperature and decreases with the increase of filler content, as shown in Fig. 10(a). According to the proton transport mechanisms, the conductivity is strongly dependent on the density of proton-conducting sites and the hydration level of the membrane [45]. Therefore, the decrease in proton conductivity of the SPEEK/TOL membranes can be partly due to the lower water uptake. Furthermore, the incorporation of unmodified titania nanoparticles dilutes the density of sulfonic acid groups and blocks the existing pathways for proton conduction in SPEEK. For the SPEEK/TOLP hybrid membranes, the proton conductivity is higher than that of pristine SPEEK membrane in the whole temperature range (Fig. 10(b)). Particularly, the proton conductivity of these hybrid membranes increases more obviously at temperatures above 50 °C. It is notable that the SPEEK/TOLP-6 hybrid membrane exhibits the highest conductivity of 0.334 S cm^{-1} at 65 °C, which is 63.7% higher than that of pristine SPEEK membrane.

The high proton conductivity of Nafion under humidified condition is attributed to the coexistence of completely separated hydrophobic/hydrophilic regions and the well-connected hydrophilic domains formed by the aggregation of sulfonic acid groups. In comparison, the channels responsible for proton and water transport in SPEEK are narrower, less separated and more branched with more dead-end "pockets" [46]. It is possible that the *in situ* formed phosphonic acid-functionalized titania nanoparticles in the polymer matrix influence the characters of the hydrophilic channels within the hydrophobic domains of SPEEK and result in improved proton conductivity. On one hand, the incorporation of phosphonic acid groups provides additional proton conduction sites inside hydrophilic channels of SPEEK. On the other hand, since phosphonic acid groups can act simultaneously as proton acceptors and donors, the homogenous distribution of phosphonic acid-functionalized titania nanoparticles may contribute to the formation of better-connected pathways for proton conduction compared with unmodified SPEEK. Besides the above effects exerted by the addition of functionalized titania phase, another reason for the increased proton conductivity is the gradually decreased interaction force between polymer chains with increasing temperature [47], leading to more water absorption and thus higher proton conductivity. For the SPEEK/TOLP-8 hybrid membrane, the decreased proton conductivity might be due to the possible agglomeration of the titania phase in the membrane.

4. Conclusion

SPEEK/phosphonic acid-functionalized titania nanohybrid membranes were successfully fabricated by an *in situ* method. Titania nanoparticles with a uniform particle size of ~50 nm were generated by hydrolysis and condensation of $TiCl_4$, and functionalized with ATMP through covalent bonds. Benefiting from the homogeneous distribution of these nanoparticles, the as-prepared hybrid membranes exhibit decreased methanol permeability as

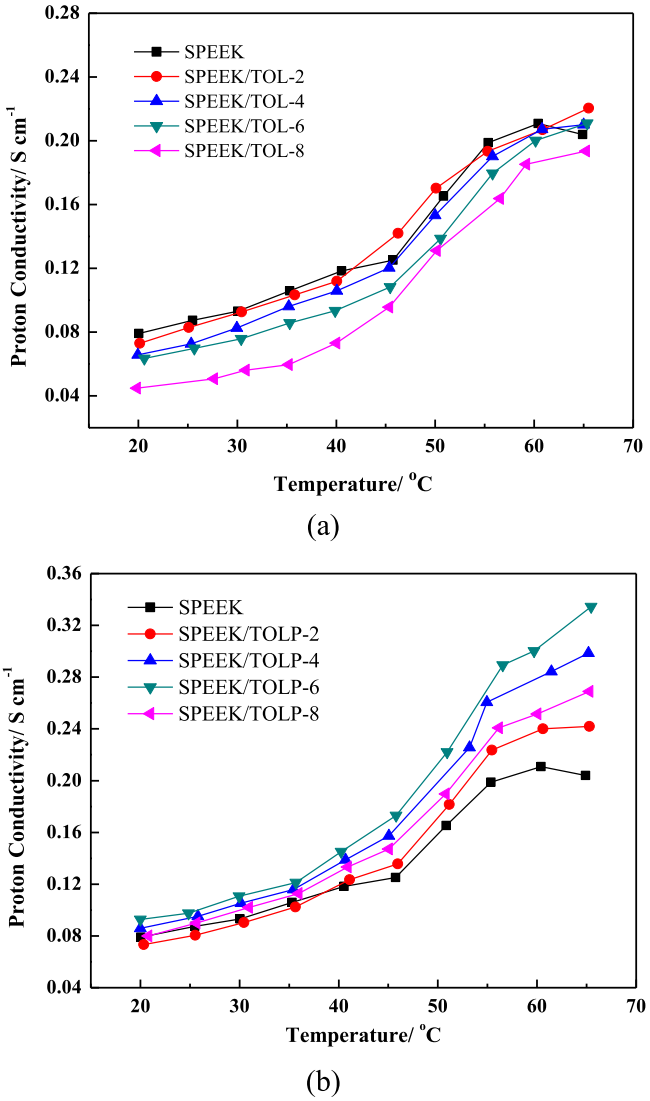

Fig. 10. Proton conductivity of the pristine SPEEK and SPEEK/TOL (a), SPEEK/TOLP (b) hybrid membranes as a function of temperature at 100% RH.

well as enhanced thermal and mechanical stabilities. Particularly, the incorporated phosphonic acid-functionalized titania nanoparticles render additional proton conduction sites and contribute to the formation of better-connected pathways for proton transfer, thus enhance the proton conductivity of hybrid membranes. The highest proton conductivity of 0.334 S cm^{-1}, which is 65.7% higher than that of pristine SPEEK membrane, is achieved at 65 °C and 100% RH for the hybrid membrane with 6 wt. % of phosphonic acid-functionalized titania nanoparticles. The developed SPEEK/phosphonic acid-functionalized titania nanohybrid membranes might have potential application prospect as proton conductors in DMFCs.

Acknowledgment

The authors gratefully acknowledge financial support from Program for New Century Excellent Talents in University (NCET-10-0623), the National Science Fund for Distinguished Young Scholars (21125627) and the Programme of Introducing Talents of Discipline to Universities (No. B06006).

Nomenclature

Symbols

X	mass ratio of inorganic fillers to SPEEK (wt. %)
W	mass of membrane (g)
A	effective membrane area (cm^2)
P	methanol permeability ($cm^2\ s^{-1}$)
S	slope of straight-line of methanol concentration in receipt compartment versus permeation time
V_A	volume of receipt compartment (cm^3)
L	membrane thickness (cm)
C_{B0}	feed concentration (mol mL^{-1})
σ	proton conductivity (S cm^{-1})
l	distance between two probes (cm)
R	membrane resistance (S^{-1})
d	dry membrane
w	wet membrane

Abbreviations

DS	sulfonation degree
SPEEK	sulfonated poly (ether ether ketone)
ATMP	amino trimethylene phosphonic acid

References

[1] F. Lufrano, V. Baglio, P. Staiti, V. Antonucci, A.S. Arico, J. Power Sources 243 (2013) 519–534.
[2] H.W. Zhang, P.K. Shen, Chem. Rev. 112 (2012) 2780–2832.
[3] V. Neburchilov, J. Martin, H. Wang, J. Zhang, J. Power Sources 169 (2007) 221–238.
[4] B.C.H. Steele, A. Heinzel, Nature 414 (2001) 345–352.
[5] M.A. Hickner, H. Ghassemi, Y.S. Kim, B.R. Einsla, J.E. McGrath, Chem. Rev. 104 (2004) 4587–4611.
[6] A. Chandan, M. Hattenberger, A. El-Kharouf, S.F. Du, A. Dhir, V. Self, B.G. Pollet, A. Ingram, W. Bujalski, J. Power Sources 231 (2013) 264–278.
[7] K.A. Mauritz, R.B. Moore, Chem. Rev. 104 (2004) 4535–4585.
[8] S.Y. Han, B.H. Yue, L.M. Yan, Acta Phys. Chim. Sin. 30 (2014) 8–21.
[9] Z. Li, G. He, B. Zhang, Y. Cao, H. Wu, Z. Jiang, Z. Tiantian, ACS Appl. Mater. Inter. 6 (2014) 9799–9807.
[10] H.R. Allcock, M.A. Hofmann, C.M. Ambler, S.N. Lvov, X.Y. Zhou, E. Chalkova, J. Weston, J. Membr. Sci. 201 (2002) 47–54.
[11] H. Steininger, M. Schuster, K.D. Kreuer, A. Kaltbeitzel, B. Bingol, W.H. Meyer, S. Schauff, G. Brunklaus, J. Maier, H.W. Spiess, Phys. Chem. Chem. Phys. 9 (2007) 1764–1773.
[12] J. Lu, H. Tang, S. Lu, H. Wu, S.P. Jiang, J. Mater. Chem. 21 (2011) 6668–6676.
[13] Y.G. Jin, S.Z. Qiao, Z.P. Xu, J.C. Diniz da Costa, G.Q. Lu, J. Phys. Chem. C 113 (2009) 3157–3163.
[14] M. Schuster, T. Rager, A. Noda, K.D. Kreuer, J. Maier, Fuel Cells 5 (2005) 355–365.
[15] S.J. Paddison, K.D. Kreuer, J. Maier, Phys. Chem. Chem. Phys. 8 (2006) 4530–4542.
[16] Y. Zhao, Z. Jiang, D. Lin, A. Dong, Z. Li, H. Wu, J. Power Sources 224 (2013) 28–36.
[17] H. Wu, W.Q. Hou, J.T. Wang, L.L. Xiao, Z.Y. Jiang, J. Power Sources 195 (2010) 4104–4113.
[18] K. Wang, S. McDermid, J. Li, N. Kremliakova, P. Kozak, C. Song, Y. Tang, J. Zhang, J. Zhang, J. Power Sources 184 (2008) 99–103.
[19] B. Muriithi, D. Loy, J. Mater. Sci. 49 (2014) 1566–1573.
[20] V. Ramani, H.R. Kunz, J.M. Fenton, J. Membr. Sci. 266 (2005) 110–114.
[21] B. Muriithi, D.A. Loy, ACS Appl. Mater. Inter. 4 (2012) 6765–6772.
[22] N.N. Krishnan, D. Henkensmeier, J.H. Jang, H.-J. Kim, Macromol. Mater. Eng. (2014) 1–11.
[23] Y.F. Li, G.W. He, S.F. Wang, S.N. Yu, F.S. Pan, H. Wu, Z.Y. Jiang, J. Mater. Chem. A 1 (2013) 10058–10077.
[24] J. Pan, H. Zhang, W. Chen, M. Pan, Int. J. Hydrogen Energy 35 (2010) 2796–2801.
[25] S. Rao, R. Xiu, J. Si, S. Lu, M. Yang, Y. Xiang, ChemSusChem 7 (2014) 822–828.
[26] B.R. Matos, R.A. Isidoro, E.I. Santiago, M. Linardi, A.S. Ferlauto, A.C. Tavares, F.C. Fonseca, J. Phys. Chem. C 117 (2013) 16863–16870.
[27] H.Q. Liang, Q.Y. Wu, L.S. Wan, X.J. Huang, Z.K. Xu, J. Membr. Sci. 465 (2014) 56–67.
[28] M.L. Di Vona, Z. Ahmed, S. Bellitto, A. Lenci, E. Traversa, S. Licoccia, J. Membr. Sci. 296 (2007) 156–161.
[29] C.Y. Yen, C.H. Lee, Y.F. Lin, H.L. Lin, Y.H. Hsiao, S.H. Liao, C.Y. Chuang, C.C.M. Ma, J. Power Sources 173 (2007) 36–44.
[30] C.C. Ke, X.J. Li, Q. Shen, S.G. Qu, Z.G. Shao, B.L. Yi, Int. J. Hydrogen Energy 36 (2011) 3606–3613.
[31] Z.W. Chen, B. Holmberg, W.Z. Li, X. Wang, W.Q. Deng, R. Munoz, Y.S. Yan, Chem. Mater. 18 (2006) 5669–5675.
[32] F. Xu, S.C. Mu, J. Nanosci. Nanotechnol. 14 (2014) 1169–1180.
[33] T. Ossiander, C. Heinzl, S. Gleich, F. Schönberger, P. Völk, M. Welsch, C. Scheu, J. Membr. Sci. 454 (2014) 12–19.
[34] J. Zhao, F. Wang, F.S. Pan, M.X. Zhang, X.Y. Yang, P. Li, Z.Y. Jiang, P. Zhang, X.Z. Cao, B.Y. Wang, J. Membr. Sci. 446 (2013) 395–404.
[35] J. Joseph, C.-Y. Tseng, B.-J. Hwang, J. Power Sources 196 (2011) 7363–7371.
[36] G. He, Y. Li, Z. Li, L. Nie, H. Wu, X. Yang, Y. Zhao, Z. Jiang, J. Power Sources 248 (2014) 951–961.
[37] H. Jensen, A. Soloviev, Z. Li, E.G. Søgaard, Appl. Surf. Sci. 246 (2005) 239–249.
[38] L. Körösi, S. Papp, I. Bertóti, I. Dékány, Chem. Mater. 19 (2007) 4811–4819.
[39] P. Krishnan, J.-S. Park, C.-S. Kim, J. Membr. Sci. 279 (2006) 220–229.
[40] M.L. Di Vona, E. Sgreccia, S. Licoccia, G. Alberti, L. Tortet, P. Knauth, J. Phys. Chem. B 113 (2009) 7505–7512.
[41] H. Wu, Y. Cao, X. Shen, Z. Li, T. Xu, Z. Jiang, J. Membr. Sci. 463 (2014) 134–144.
[42] E. Sgreccia, J.F. Chailan, M. Khadhraoui, M.L. Di Vona, P. Knauth, J. Power Sources 195 (2010) 7770–7775.
[43] A. Reyna-Valencia, S. Kaliaguine, M. Bousmina, J. Appl. Polym. Sci. 98 (2005) 2380–2393.
[44] K.D. Kreuer, S.J. Paddison, E. Spohr, M. Schuster, Chem. Rev. 104 (2004) 4637–4678.
[45] G.W. He, Z.Y. Li, Y.F. Li, Z. Li, H. Wu, X.L. Yang, Z.Y. Jiang, ACS Appl. Mater. Inter. 6 (2014) 5362–5366.
[46] A. Iulianelli, A. Basile, Int. J. Hydrogen Energy 37 (2012) 15241–15255.
[47] I. Colicchio, F. Wen, H. Keul, U. Simon, M. Moeller, J. Membr. Sci. 326 (2009) 45–57.